Magnetic properties of monodomain Nd-Fe-B-C nanoparticles

E. M. Brunsman, J. H. Scott, and S. A. Majetich[a)]
Department of Physics, Carnegie Mellon University, Pittsburgh, Pennsylvania 15213-3890

M. E. McHenry and M.-Q. Huang
Department of Materials Science and Engineering, Carnegie Mellon University, Pittsburgh, Pennsylvania 15213-3890

Nanoparticles of Nd-Fe-B-C with their crystal structure similar to the $Nd_2Fe_{14}B$ phase were generated in a carbon arc. With an average diameter of less than 40 nm, they are monodomain. They have a smaller room-temperature coercivity than would be predicted from the bulk magnetocrystalline anisotropy. However, their coercivity is greater than was previously observed in particles <5 μm prepared by spark erosion. While the carbon arc process is useful for making small carbon-coated particles which resist oxidation, here dispersion of excess Nd in the carbon matrix results in a significant paramagnetic signal. The dc demagnetization curves enable the paramagnetic and ferromagnetic contributions to be distinguished. © *1996 American Institute of Physics.* [S0021-8979(96)40308-8]

I. INTRODUCTION

Fine particle magnetism has been an active field for many years.[1–3] Experimental support for this theory has been obtained for a variety of ferromagnetic fine particles.[4] However, since this time there have been significant developments both in permanent magnet materials and in fine particle synthesis. Here we combine two of these breakthroughs, the high magnetocrystalline anisotropy alloy neodymium iron boron and the carbon arc process[5] for preparing nanocrystals,[6] and analyze the magnetic properties of the resulting monodomain particles.

Bulk neodymium iron boron magnets have the highest known energy product of any permanent magnet material.[7] This ternary alloy is quite complex. Boron is present to stabilize the hard magnetic phase, tetragonal $Nd_2Fe_{14}B$.[8] Sintered magnets frequently have a secondary α-Fe phase of approximately 10 nm thickness at the grain boundaries,[9] which may be significant in the oxidation which plagues these materials. At low temperatures, bulk $Nd_2Fe_{14}B$ also undergoes a spin reorientation transition at 135 K.[10] The magnetic properties of the related materials, $Nd_2Fe_{14}B_{.5}C_{.5}$ and $Nd_2Fe_{14}C$, have also been reported.[11]

Several groups have prepared micron-sized particles of Nd-Fe-B alloys, by spark erosion in liquid argon,[12] by ball milling,[13] and by heat treatment of metal and oxide powders.[14] In all of these materials the particle sizes were on the order of microns, and they therefore contained multiple magnetic domains. The coercivities measured were significantly smaller than in the bulk material.

Monodomain particles of Nd-Fe-B-C are of interest to test the model of size-dependent coercivity.[15] The maximum size for a single magnetic domain has been estimated at $\sim$200 nm for $Nd_2Fe_{14}B$.[16] The carbon arc process has been applied to a variety of metals and alloys to prepare nanoparticles in the 5–50 nm size range, well below the single domain threshold. The carbon coating of the nanoparticles is also an advantage in preventing oxidation. Cobalt particles made by this method have been boiled in sulfuric acid without reaction.[17] We have recently demonstrated the use of electron spectroscopic imaging to obtain elemental maps on a nanometer scale,[18] which could enable us to detect nanometer-scale phase separation in this alloy. With this new approach to synthesis and and a new tool to characterize chemical inhomogeneity, we sought to understand the behavior of these monodomain magnets.

II. EXPERIMENT

Nanoparticles embedded in a carbon matrix were prepared by a variation of the Huffman–Krätschmer carbon arc process.[5] To make the nanoparticles, a composite anode was made from graphite and 30 wt % Nd-Fe-B (Crucible, Inc.), with dextrin as a binder. Though this method has been used to prepare other materials with up to 70 wt % metal,[19] a 30 wt % metal fraction was studied here. The composite anode was combined with a graphite cathode in a carbon arc (30 V dc, 100 A, 500 Torr He), and vaporized. The nanoparticles were collected as a powder from the reactor walls.

The nanoparticle morphology was determined through a combination of transmission electron microscopy (TEM) and x-ray diffraction (XRD) measurements on as-prepared and annealed powder samples. Electron spectroscopic imaging (ESI) of an annealed sample was done with a Gatan Imaging Filter attachment to a JEOL 4000 EX electron microscope. In this technique a combination of high-resolution imaging and electron energy loss spectrometry is used to generate elemental maps.

For magnetic measurements, the powders were dispersed in epoxy and placed in a Quantum Design SQUID magnetometer at fields between ± 5 kOe for temperatures ranging

a)Author to whom correspondence should be addressed.

 0021-8979/96/79(8)/5293/3/$10.00

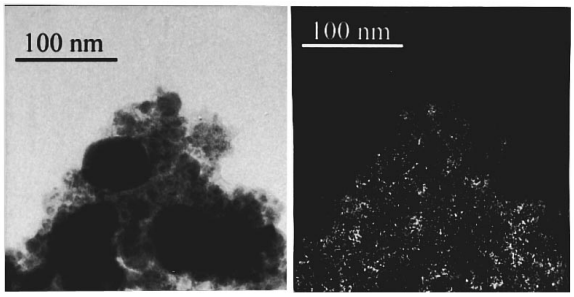

FIG. 1. Left: TEM of carbon-coated Nd-Fe-B-C nanoparticles. Dark spheroidal regions are the nanoparticles and smaller spheres are part of the amorphous carbon matrix. Right: electron spectroscopic imaging of the same sample, showing the distribution of Nd. The corresponding Fe map shows that only the nanoparticles contain iron.

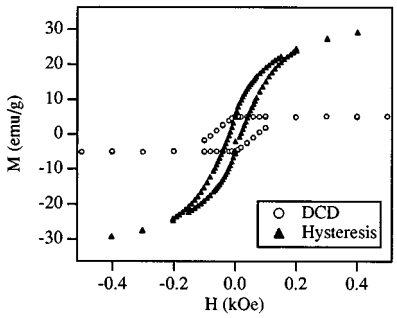

FIG. 2. Ordinary hysteresis loop for Nd-Fe-B-C nanoparticles, and dc demagnetization curve for the same sample.

from 2 to 300 K. The diamagnetic contributions of the epoxy and carbon matrix were measured separately and subtracted from the magnetization data. Due to the possibility of additional paramagnetic contributions from Nd carbides, the dc demagnetization (DCD) curves[20] were also measured. Here the sample was first saturated and then subjected to an increasingly negative field. The remanent magnetization, M_r, is measured after the field is removed.

III. RESULTS AND DISCUSSION

The carbon arc process generated gram quantities of spherical nanoparticles well below the monodomain threshold. The particles were embedded in an amorphous carbon matrix, and followed a log-normal size distribution, with an average radius of 18.2 nm and a standard deviation of 1.9 nm.

The sample was annealed in argon for 12 h at 900 °C, without increasing the average particle size determined by TEM. Several x-ray diffraction peaks similar to those in the $Nd_2Fe_{14}B$ phase emerged: (410), 100%, $2\theta=42.4°$; (411), 64%, 43.5°; (314), 77%, 44.6°, though not all of the prominent features were detected. No evidence of α-Fe, NdC_2, or $Nd_3Fe_{20}C_x$ (Ref. 21) was observed. Nominal $Nd_2Fe_{14}C$ is actually a mixture of rhombohedral $Nd_2Fe_{17}C_x$ and α-Fe,[11] and is inconsistent with our data. The most likely structure is an alloy similar to $Nd_2Fe_{14}B$, but containing a mixture of B and C.

Electron spectroscopic imaging was used to obtain Nd (Fig. 1) and Fe maps in an annealed sample. While the iron was localized within the nanoparticles, we found that Nd was distributed throughout both the particles and the matrix. In the matrix, it presumably took the form of NdC_2 or Nd_2C_3 clusters too small to be detectable by XRD. These species are paramagnetic and therefore contribute to the overall magnetization, but not to the remanence or coercivity. We saw no evidence of a Nd-deficient layer near the nanoparticle surface as found in the bulk material, or for a mixture of Nd-Fe and α-Fe phases. No oxygen was detected in these samples, verifying that the carbon coating protects the nanoparticles from oxidation. While this technique is extremely useful for measuring elemental abundances on a nanometer scale, this is not yet a quantitative technique. It could not be used to determine the exact stoichiometry, because the carbon signal could arise from either dissolved carbon in the nanoparticles or from the carbon coating which surrounds them.

The hysteresis loops for the Nd-Fe-B-C nanoparticles show coercivity even at room temperature (Fig. 2), but H_c is considerably smaller than would be predicted from the particle size and the room-temperature anisotropy of the bulk material. For a sample prepared from 30 wt % Nd-Fe-B starting material, $M_s=49.5$ emu/g, $M_r=14.2$ emu/g, and $H_c=830$ Oe at 5 K. The switching field distribution showed no indication of multiple phases with widely differing coercivities. The remanent magnetization dropped sharply with temperature up to approximately 45 K, and continued to drop more slowly up to room temperature. This contrasts with a maximum in the magnetization at ~100 K in bulk $Nd_2Fe_{14}B_{0.5}C_{0.5}$, which has a spin reorientation temperature of 128 K.[11]

The difference between the saturation and remanent magnetizations is greater than the factor of two expected for random ordering, but consistent with a large paramagnetic contribution from the neodymium carbide clusters. DCD measurements (Fig. 2) showed similar values for M_r, but smaller values of M_s and larger values of H_c (1500 Oe at 5 K) because the paramagnetic contributions were absent. The magnetization reversal of the paramagnetic fraction before that of the ferromagnetic particles reduces the overall magnetization and shifts the field for which $M=0$, thereby reducing the measured coercivity. Efforts to model the DCD curves are underway.

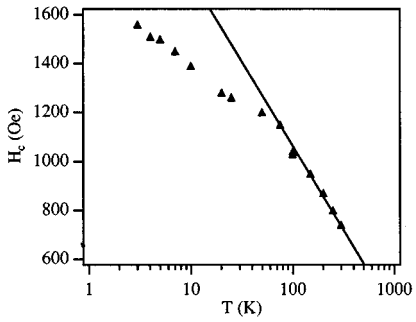

FIG. 3. The dc demagnetization curve coercive field as a function of temperature. Fit to high-temperature data indicates an (A-$BT^{0.28}$) dependence, where A and B are constants.

In spherical particles of $Nd_2Fe_{14}B$, magnetocrystalline anisotropy is expected to dominate the shape anisotropy in determining the field required for magnetization reversal. Stoner–Wohlfarth theory[2] predicts that below the blocking temperature, T_B, the lowest temperature at which the coercivity equals zero, H_c will obey at $T^{1/2}$ power law. Experimentally we observe a $T^{0.28}$ dependence of the measured coercivity (Fig. 3) above 75 K and a $T^{0.17}$ dependence below it. Because the anisotropy energy density of bulk $Nd_2Fe_{14}B_{0.5}C_{0.5}$ changes sign at low temperature,[11] the Stoner–Wohlfarth model cannot be used to quantitatively interpret the results. A temperature dependence T^x with $x<0.5$ has been observed in nanocrystalline materials with interacting grains, and here we may have some interactions between nanoparticles. Studies in lower abundance samples are underway.

IV. CONCLUSIONS

High coercivity monodomain nanoparticles of Nd-Fe-B-C in a carbon matrix have been prepared by the carbon arc process. Structural and chemical characterization indicates the presence of a phase similar to that of $Nd_2Fe_{14}B$, probably containing carbon. Neodymium was found to be dispersed throughout the carbon matrix, leading to a significant paramagnetic contribution to the magnetic results, and making dc demagnetization measurements essential for measuring the magnetic behavior of the nanoparticles. While the measured coercivity is greater than previously reported for micron-sized particles, it is still far below the value predicted from the bulk anisotropy energy density.

ACKNOWLEDGMENTS

The NSF has supported this research through Grants No. DMR-9258450 (S.A.M.), No. DMR-9258308 (M.E.M.), and No. DMR-95000313 (S.A.M. and M.E.M). This work is also based (in part) upon work supported by the NSF under Grants No. ECD-8907068 and No. DMR-9403621. We would like to thank Dr. A. Kim of Crucible, Inc. for providing Nd-Fe-B powder starting material. The participation of the CMU Buckyball Project members have been extremely helpful.

[1] L. Néel, Ann. Geophys. **5**, 99 (1949); C. R. Acad. Sci. **228**, 664 (1949).
[2] E. C. Stoner and E. P. Wohlfarth, Philos. Trans. R. Soc. London **240**, 599 (1948).
[3] W. F. Brown, Jr., J. Appl. Phys. **29**, 470 (1958); **30**, Suppl. 130S (1959).
[4] F. E. Luborsky, J. Appl. Phys. **32**, Suppl. 171S (1961).
[5] W. Krätschmer, L. D. Lamb, K. Fostiropoulos, and D. R. Huffman, Nature **347**, 354, (1990).
[6] S. A. Majetich, J. O. Artman, M. E. McHenry, N. T. Nuhfer, and S. W. Staley, Phys. Rev. B **48**, 16845 (1993).
[7] R. A. McCurrie, *Ferromagnetic Materials: Structure and Properties* (Academic, New York 1994), Chap. 5, p. 278.
[8] R. A. McCurrie, Ferromagnetic Materials: Structure and Properties (Academic, New York, 1994), Chap. 5, p. 271.
[9] S. Hirosawa, K. Tokuhara, Y. Matsuura, H. Yamamoto, S. Fujimura, and M. Sagawa, J. Magn. Magn. Mater. **61**, 363 (1986).
[10] J. Hu, X. C. Kou, and H. Kronmüller, Phys. Status Solidi A **138**, K41 (1993).
[11] X. C. Kou, X. K. Sun, Y. C. Chuang, R. Grössinger, and H. R. Kirchmayr, J. Magn. Magn. Mater. **80**, 31 (1989).
[12] H. Wan and A. E. Berkowitz, Scr. Metall. Mater. **32**, 1827 (1995).
[13] S. Ram and J. C. Joubert, J. Appl. Phys. **72**, 1164 (1992).
[14] A. Ahmad, P. J. McGuiness, and I. R. Harris, IEEE Trans. Magn. **26**, 2625 (1990).
[15] G. Herzer, IEEE Trans. Magn. **26**, 1397 (1990); J. Magn. Magn. Mater. **112**, 258 (1992).
[16] K. D. Durst and H. Kronmüller, J. Magn. Magn. Mater. **59**, 86 (1986); **68**, 63 (1987).
[17] S. A. Majetich, J. H. Scott, E. M. Brunsman, M. E. McHenry, and D. C. Winkler, *Fullerenes: Physics, Chemistry, and New Directions VII*, edited by R. S. Ruoff and K. M. Kadish (The Electrochemical Society, Pennington, NJ, 1995), p. 584.
[18] J. H. J. Scott and S. A. Majetich, Appl. Phys. Lett. (unpublished)
[19] J. H. Scott and S. A. Majetich, Phys. Rev. B **52**, 12564 (1995).
[20] S. Gangopadhyay, G. C. Hadjipanayis, C. M. Sorensen, and K. J. Klabunde, IEEE Trans. Magn. **29**, 2619 (1993).
[21] L. Sheng, Z. Lui, Z. Guowei, P. Xiedi, J. Wei, and H. Wenwang, IEEE Trans. Magn. **23**, 3095 (1987).